

Neuroimaging patterns of neuronal-glia tumors associated with focal epilepsy in children

Khalilov V.S.^{*,1,2}, Kholin A.A.¹, Zavadenko N.N.¹, Gazdieva Kh.Sh.¹

¹ Department of Child Neurology, Neurosurgery and Medical Genetics, Pediatric Faculty, N.I. Pirogov Russian National Research Medical University, Moscow

² Department of Magnetic-Resonance Tomography, Central Children's Clinical Hospital of Federal Medical-Biological Agency, Moscow

*Correspondence: V.S. Khalilov, Department of Magnetic-Resonance Tomography, Central Children's Clinical Hospital of Federal Medical-Biological Agency, Moscow

Email: khalilov.mri@gmail.com

Keywords

neuronal-glia tumours; drug-resistant epilepsy; neuroimaging

© 2020 Khalilov et al; licensee JICNA

Submitted: 16.11.2018

Accepted: 30.05.2019

Published: 05.01.2020

This is a PDF file of a manuscript that has been accepted for publication. As a service to our customers we are providing this early version of the manuscript. The manuscript will undergo typesetting, and review of the resulting proof before it is published in its final citable form. Please note that during the production process errors may be discovered which could affect the content, and all legal disclaimers that apply to the journal pertain.

Abstract

Our report intends to analyse the specificity of certain magnetic resonance patterns which occur in imaging of neuronal-glia tumours associated with epilepsy in children.

Materials and methods

Thirty-three children suffering from neuronal-glia tumours associated with symptomatic epilepsy (aged from five months to 17 years) were examined and treated from 2007 to 2017; prospective follow-up lasted from one to eight years. MRI was performed by means of an apparatus with magnetic field induction of 1.5 and 3.0 Tesla before and after surgery. A high-resolution MRI scan was applied in accordance with the epileptic scanning protocol. Anaesthesia included the method of sevoflurane sedation.

Results

Dysembryoplastic neuroepithelial tumours (DNETs) – confirmed histopathologically – were revealed in 18 children; gangliogliomas (GGs) were revealed in 15 children. Histological analysis revealed the evidence of both DNET and GG in one tumour site in two patients. Six patients showed a histopathologically confirmed association of neuronal-glia tumours with focal cortical dysplasia (FCD) type IIIb by I. Blumcke *et al.* classification (2011). Verification of the neoplastic process on MRI results was complicated in 12 patients. Twenty-one (21) patients showed specific MRI signs of the tumours being of neuronal-glia origin as described in the literature: a cortical localisation, a 'triangular' shape, a 'comet tail' symptom, and a 'soap

bubble' pattern. Based on tractography (DTI) and fractional anisotropy (FA), the path's displacement without the distraction of the fibres' integrity was observed in four patients with DNET and two patients with GG. Peritumoral hyperintensity of the signal, the abnormality of gray-white differentiation and cortical organisation led to us suggesting a combination with FCD IIIb in nine patients. One case of DNET and four cases of GGs turned out to be contrast-positive. The localisation was predominantly temporal. Reliable signs of a neoplastic process in the differential diagnosis were the contrast enhancement and continued growth led to the adjacent bone tissue remodeling. However, in some cases, differentiation of DNETs, GGs and FCD IIb having a number of similar MRI signs was not possible until the histological diagnosis was made

Introduction

Approximately 20–30% of progressive drug-resistant paediatric epilepsy cases are caused by tumours of neuroepithelial tissue with a predominance of neuronal-glioma tumours [1]. Epilepsy is usually a primary manifestation, and in some cases, the only manifestation of these tumours. Thus, children may retain higher cerebral functions, i.e., maintain normal cognitive abilities, or demonstrate a specific developmental delay or deterioration associated with a particular form of epilepsy, including behavioural disorders. DNETs and GGs along with FCD are the most common causes for epileptic surgery in children [2, 3]. The identification of these tumours is important to determine the treatment strategy and prognosis. They are benign tumours but they may have similarities with more aggressive ones. DNETs and GGs may not demonstrate typical neuroradiological signs of a tumour, and a differential diagnosis of these tumours, and even, in some cases, verification of the neoplastic process, requires a prolonged dynamic observation, and is known to be complicated [4, 5, 6]. In the present study, the authors have tried to collect all the most specific neuroimaging patterns for DNET and GG as described in the literature and to apply them when analysing the images obtained from the studied group of patients.

The purpose of the study

The purpose of the study is to analyse MRIs received during pre-surgical neuroimaging of neuronal-glioma tumours associated with epilepsy in children, in order to reveal the presence of specific signs.

Materials and methods

From the total group of 52 patients with supratentorial tumours operated on for drug-resistant epilepsy from 2007 to 2018, 33 children with histopathologically confirmed neuronal-glioma tumours of DNET and GG underwent a complete assessment program, and surgical treatment and histological verification of the diagnosis were identified for them. The patients' age varied from five months to 18 years with postoperative observation up to eight years.

Phacomatoses were the exclusion criteria, so patients with tuberous sclerosis and type I neurofibromatosis were not included in the study, despite the presence of neuroepithelial and glioma tumours of hemispheric localisation.

Upon admission to the hospital, each patient's medical history was taken; abnormalities in the neurological status were recorded in the protocol. Each patient participating in the study underwent a dynamic brain MRI with contrast enhancement on admission to the hospital, before and after surgery. Video-EEG monitoring of night or day sleep was performed, and depending on the case, patients underwent pre-surgical video-EEG monitoring and intraoperative electrocorticography (ECoG). The ECoG was performed before, during and after surgery. In the postoperative period, the neurological status of the patient was studied, and a postoperative MRI examination of the brain with contrast matter and dynamic MRI control were performed after six months.

In the presence of a history of epilepsy, postoperative video-EEG monitoring and dynamic control of EEG were carried out. MRI was performed by means of 1.5 and 3.0 Tesla apparatus. The standard examination with a highly inductive MR system (1.5 T) was conducted with a slice thickness of 4 or 5 mm (depending on the size of the patient's head), a step of 2 mm, and an image matrix of 512 x 512 pixels, and included various modes of T1 and T2 SE, FSE, FLAIR, DW and GRA T2 visualisation. Applied high-resolution MRI with a minimum thickness of the scan slice of no more than 1.7 mm, a minimum scanning step of 0.1 mm, and the use of special hippocampal positioning of the slices when the coronal section is oriented as a perpendicular to the long axis of the hippocampus. T2 fast spin-echo in axial and coronal slices as well as T1 IREPI were used.

A modified epileptic scanning protocol was used on a super inductive MRI system (3.0 T). The protocol included pulse sequences T2 PROPELLER, FLAIR in the axial and coronal planes, FSPGRBRAVO, T1 SE, DWI, SWAN, DTI and ASL. Anaesthesia is used for patient immobilisation (with sevoflurane as the method of sedation). Anaesthesia apparatus *Anestiva-5*-monitoring was performed by means of *Datex-Ochmeda 5/S*. Intravascular contrast enhancement with semi-molar agents (Gadopentetatedimeglumine; Magnevist; Schering A. G.) and one-molar agents (Gadobutrol 1.0; Gadovist 1.0, Schering A. G.) were used.

All patients underwent dynamic routine video-EEG monitoring in the state of wakefulness and sleep at least three times, performed before and after surgery; intensive preoperative video-EEG monitoring under the scheme 10-10, as well as intraoperative corticography (pre-resection, and at least one post-resection ECoG record).

The examinations were carried out by means of video-EEG 'Encephalan-video' RM-EEG-19/26 'Encephalan-RM' monitoring apparatus ('Medikom MTD', Taganrog, Russia), 'Biola NS 425' apparatus ('Biola', Moscow, Russia), 'Grass-Telefactor Beehive' and 'Aura' apparatuses (USA). Intensive preoperative video-EEG monitoring under the scheme 10-10 was performed on 'BiolaNS432' and 'NS450' electroencephalographs ('Biola', Moscow, Russia), as well as 'Nihon Kohden 1200K' (Japan).

ECoG was performed with sterile striped 6- and 10-pin subdural electrodes (AD-TECH, USA). Histological tissue samples of patients were fixed in buffered formalin and poured into paraffin; thickness of the slices was 3 μm . In all cases, the samples were coloured with hematoxylin and eosin; immuno-histochemical examination was performed with the following antibodies to: glial fibrillar acidic protein (clone EP672Y), synaptophysin (clone MRQ-40), neurofilaments protein (clone 2F11), vimentin (clone V9, CD34 (clone QBEnd/10), Ki-67 (clone 30-9) and general cytokeratin (clone AE1/AE3&PCK26).

The technique of immunophenotyping was provided by the detection system 'Ultra View Universal DAB Detection Kit'. The detection system and all antibodies used were produced by means of Ventana Medical Systems, Inc., USA. The diagnoses were accomplished in accordance with the WHO classification of central nervous system (CNS) tumours (2007).

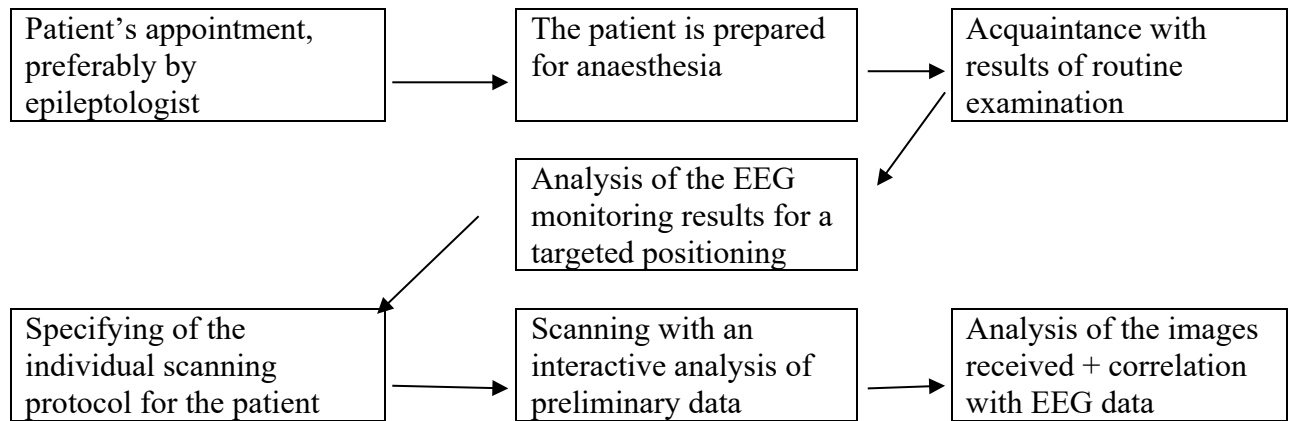


Figure 1. The algorithm of the pre-surgical assessment in cases of unclear focal abnormalities in regions of the cortical plate difficult to access, associated with drug-resistant epilepsy.

Results

Histopathologically confirmed DNETs and GGs were revealed in 18 and 15 patients, respectively. Two of the patients were children and both showed histological signs of DNET and GG in one tumour site, which coincides with the literature data [7]. In six cases the association of neuronal-glial tumours with focal cortical dysplasia – FCD type IIIb by I. Blumcke *et al.* classification (2011) [8] – was revealed and histopathologically confirmed. In 2011 the new pathomorphological classification proposed for different variants of FCD was published and approved by ILAE [8]. According to this classification, FCD type I is characterised only by various disorders of histoarchitectonics of the cortex and consists of three subtypes (Ia, Ib, Ic); type II necessarily includes cytological abnormalities (dysmorphic neurons and/or balloon cells) and is divided into subtypes IIa and IIb. In addition, there is a complex type of FCD type III, which includes any (both histological and cytological characteristics of types I and II, respectively) cortex dysplasia, combined with the presence in the perifocal region of another pathological substrate, which itself can cause pharmaco-resistant epilepsy. The combination of the neoplastic process with FCD adjacent to the tumour is referred to as FCD IIIb, according to the ILAE classification of 2011 [8].

One (1) DNET and four (4) GGs turned out to be contrast-positive when a one-molar agent was used. It should be noted that contrast enhancement was carried out for most children with semi-molar agents, while a significant increase of accumulation was observed in one patient (Fig 5 – b, c).

Verification of the neoplastic process on the results of the neuroradiological investigation was impeded in 12 patients on admission (Fig. 2). In one case, we failed to diagnose the neoplastic process by neuroimaging; differentiation was carried out between the brain tumour and CNS infection consequences. Having conducted the prolonged dynamic follow-up, we were able to make a reliable diagnosis only after an extended biopsy (Fig. 2 – g, h).

According to neuroimaging data, the majority of DNETs could be divided into three types: type 1 – cystic/multi-cystic; type 2 – nodular; and type 3 – dysplastic (diffuse, poor tumour/tissue differentiation; blurring of gray-white matter differentiation) [8]. However, when comparing the results of the histological examination with MRIs, we obtained a similar gradation of radiological signs in most patients with GGs (Fig. 2) [9]. The fact that the MRI of GGs may be similar to the MRI of DNETs was mentioned by Fernandez *et al.* in 2003 [2], but the authors describe a number of MRI specific attributes as characteristic traits of the DNETs, in particular.

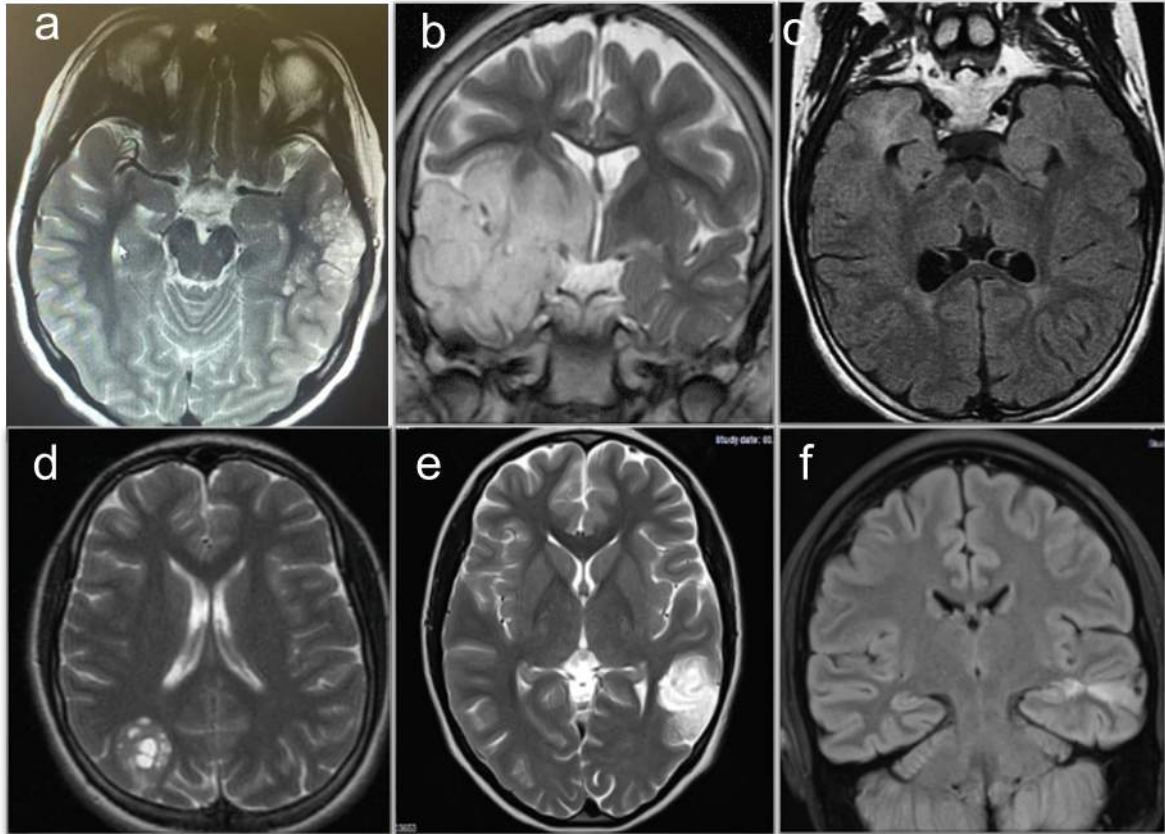


Figure 2. The possible structural architectonics of DNET and GG according to the visualisation data.

Top row: DNET: (a) multi-cystic type, (b) nodular type, and (c) diffuse (dysplastic) type. In the latter case, the differentiation was performed between the effects of hypoxic-ischaemic injury and FCD. A histological diagnosis of DNET+FCD IIIb of the right temporal lobe (ILAE classification of FCD, 2011 [8]).

Bottom row: GG: (d) the multi-cystic structure with the presence of the main cyst is determined; (e) the nodular gyriform pattern without perifocal reaction and mass effect on the posterolateral segments of the left temporal lobe, (f) contrast-negative zone of signal enhancement in FLAIR weighted imaging (WI) in the media-base parts of the left hippocampus, smoothing gray-white differentiation. Brain convolutions are represented as locally thickened, their pattern is disorganised. Trans-mantle pattern towards homolateral ventricle is notable. Histological diagnosis: GG+DNET+FCD IIIb of the left temporal lobe (ILAE classification of FCD, 2011 [8]).

On the routine MRI, the characteristic neuroradiological signs of neuronal-glial tumours described in the literature were found in 17 patients (Fig. 3). Localisation of tumours was predominantly temporal in 16 cases, which corresponds to the literature data [4-7]. Detailed results are presented in Table 1.

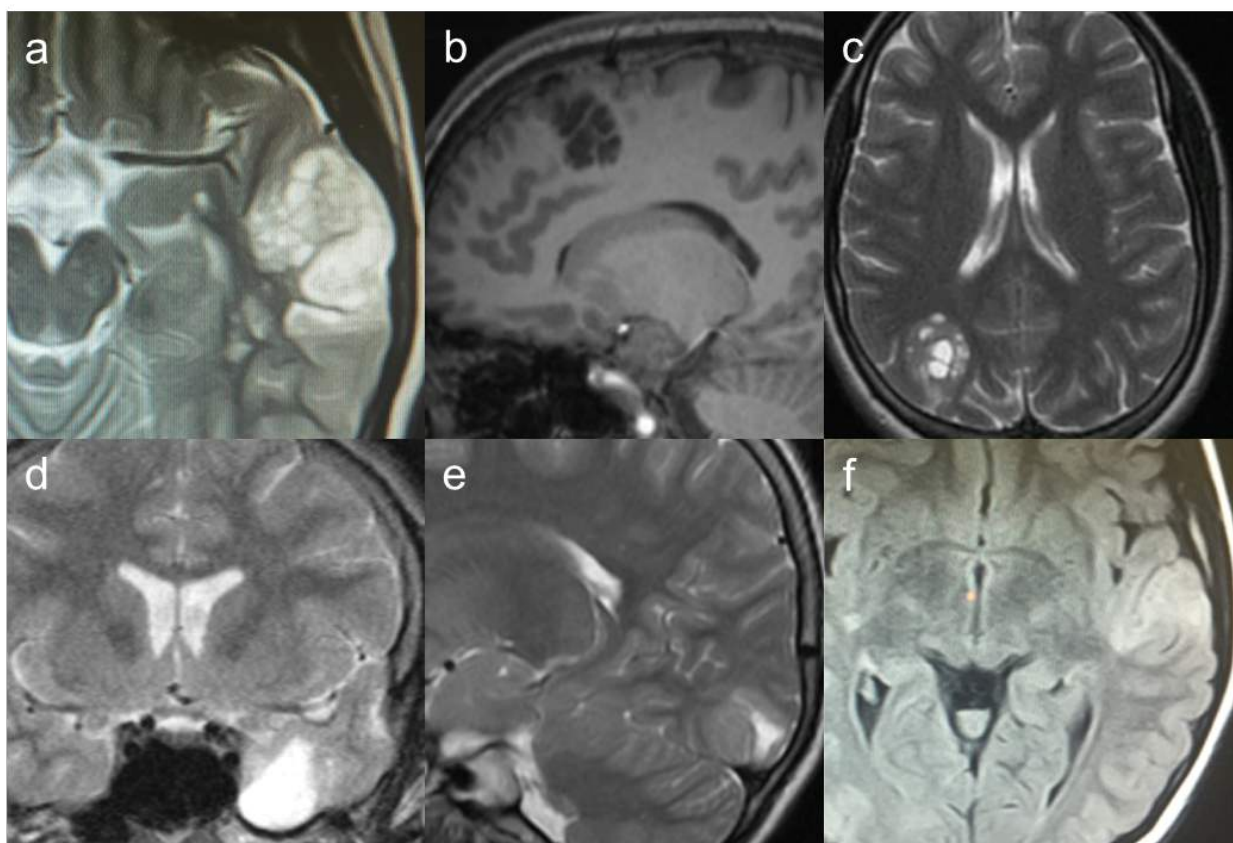


Figure 3. Visualization patterns specific to DNET and GG.

Top row: Enlarged heterogeneous gyrus, with focal increase of MRI signal in T2 and FLAIR WI with well visualised delicate structures, like parting walls, which can be seen inside the lesion; it creates an image similar to a soap bubble (a, b, c, d). In almost all cases of multicystic structure visualisation, the main, larger cyst surrounded by many small ones was seen in GG (c, d).

Bottom row: In almost every case, the focal lesion volume exceeded the normal thickness of the cortex, so that it was wedged into the adjacent layer of the white matter (e, f, g, h). The masses were at their widest in the convex part of the cortical plate, tapering towards the white matter and forming a kind of triangular pattern, clearly visible on the frontal slices in the T2 and FLAIR WI (e, f, g).

Reliable signs of the neoplastic process, such as contrast enhancement, remodeling of the underlying bone plate and changes in the configuration and size of cortical substrates of unknown etiology presupposed the presence of tumours in 11 patients under dynamic control (Fig. 4). In some cases of diffuse growth, only the presence of contrast enhancement or its appearance during the follow-up presupposed the neoplastic origin of morphological changes (Fig. 4 – g, d, e).

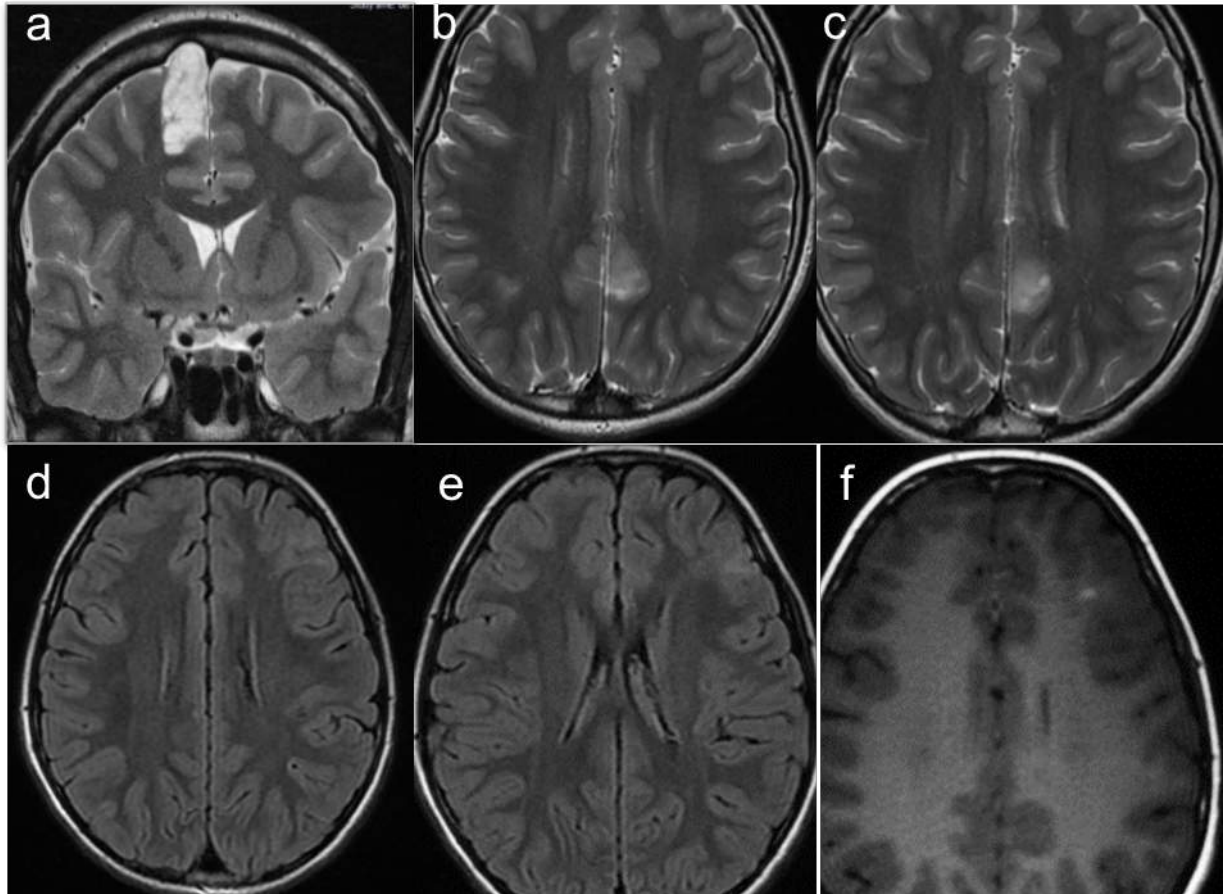


Figure 4. Reliable signs of the neoplastic process.

Top row. (a) Bone remodeling at the border with a pathological cortical focus. As a rule, an uneven thinning of the underlying portion of the bone plate is observed; this uneven thinning is clearly visible in computed tomography (CT) images, and in the coronary plane on the MRI in T2. (b, c) Extended growth. Structure transformation of the intracortical focal lesion in the parasagittal parts of the left parietal lobe (rise of additional cystic inclusions), without any change in the size and configuration, with dynamic control in the period of 6–12 months.

Bottom row. (d, e, f) Contrast enhancement. Diffuse form of GG+FCD IIIb, differential diagnosis with FCD IIb, in the absence of typical neuroradiological signs of the focal lesion and the abovementioned signs; only contrast enhancement may indicate the neoplastic origin of morphological abnormalities.

DTI and FA have become available with the purchase of a superinductive MRI system, and were performed in only seven children, in whom DNET and GG were confirmed during the follow-up. In six patients, similar signs of the bias and divergence of tracts without disruption of the integrity of their fibres and signs of infiltration were revealed (Fig. 5).

In one more case of GG transformation, the contrast enhancement and signs of infiltration of the displaced tracts were noticed during dynamic control (Fig. 5b). Using high resolution MRI and epileptic scanning protocol, the combination of several specific signs was revealed. Cortical localisation and triangular configuration of the focal lesion, the soap bubble pattern, and changes of the underlying bone plate presupposes the presence of a neuronal-glioma prior to its histological confirmation in 21 of 33 patients.

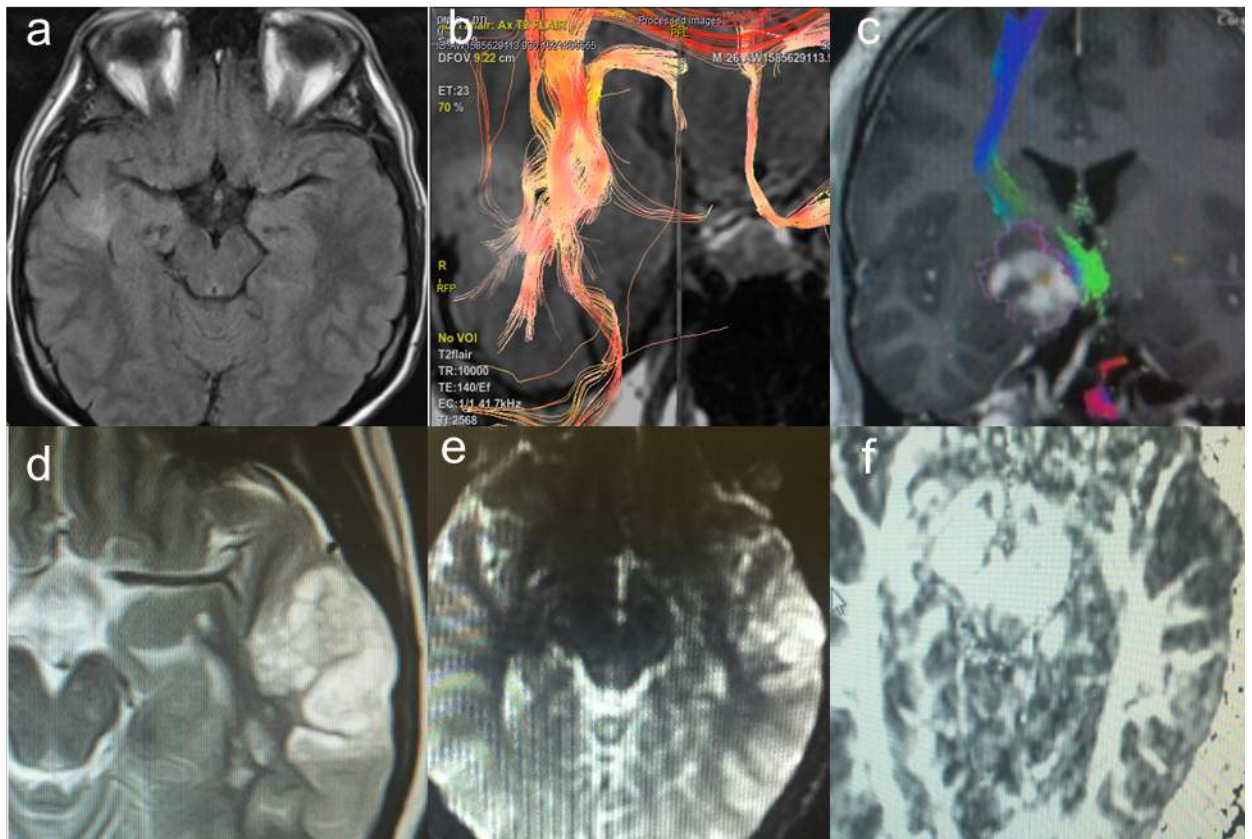


Figure 5. Assessment of the neoplastic process malignancy degree based on the DTI and FA results.

Top row: (a, b) GG of the lateral parts of the right temporal lobe, the deviation of tracts along the boundaries of formation, without signs of damage or infiltration. (c) GG of the right hippocampus at the stage of transformation into a more malignant form, as also evidenced by the contrast enhancement. DTI determines the deviation of tracts with initial signs of infiltration.

Bottom row: (d, e, f) Assessment of peritumoral white matter in the DNET of lateral parts of the left temporal lobe, according to FA data, determines their integrity.

A differential diagnosis in the presence of one or more of the above patterns, the absence of contrast enhancement and dynamic transformation of the intracortical lesion, was performed between neuronal-gliol tumours DNET, GG and FCD of the type IIb in 11 cases (Fig. 6a, b). Then with the presence of indirect signs and peculiarities of MRIs, the diffuse astrocytomas Grade I-II and oligodendrogliomas were considered. As a rule, tumours with progressive growth have changed in size and shape on the 1–2 follow-up dynamic MRIs, with a time interval of six months. Abnormalities in the peritumoral cortical plate presupposed the presence of FCD IIIb in nine children (Fig. 4e, f, g, h); with this, six cases were confirmed histopathologically (Tab. 1).

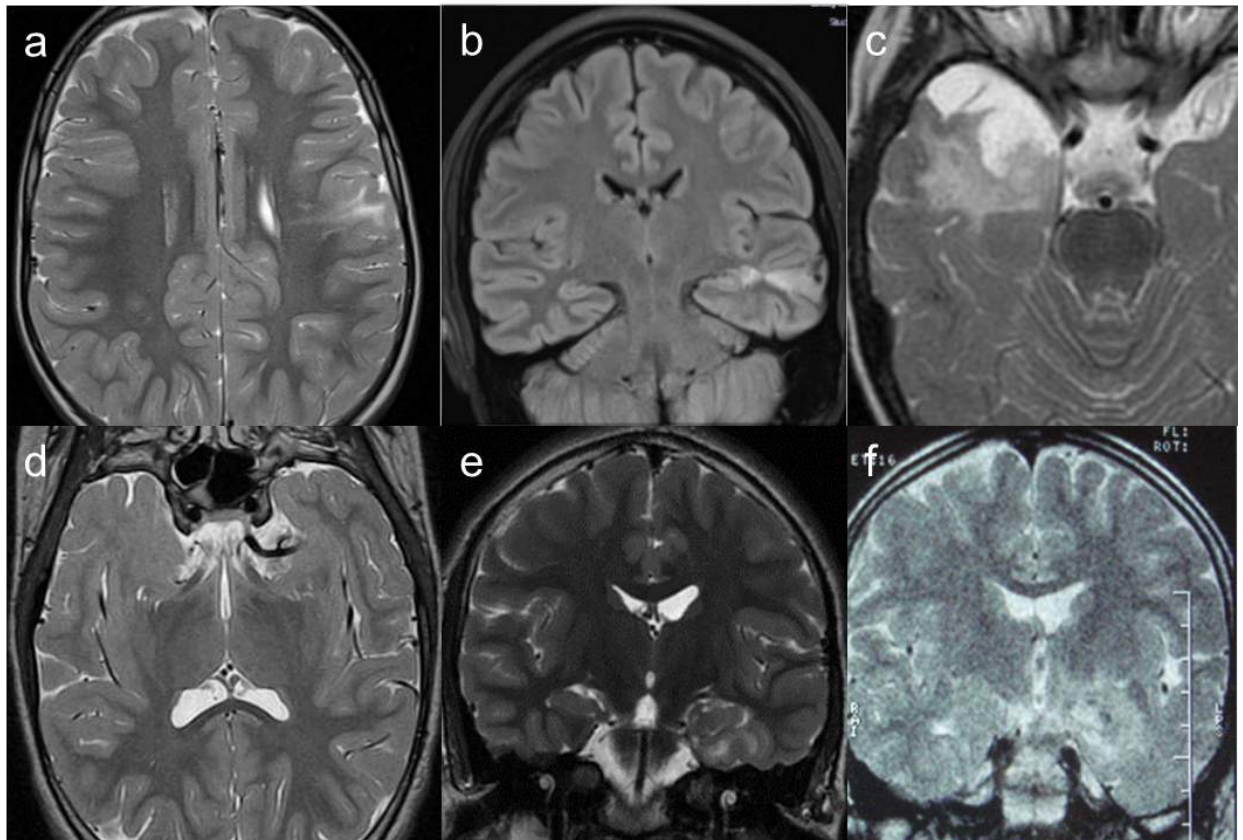


Figure 6. Examples of differential diagnosis and FCD association.

Visualisation of trans-mantle pattern in (a) FCD IIb and (b) GG + DNET + FCD IIIb. The main lesion is located in the basement membrane of the cortex, spreading with hyperintensional cord in the white matter, to the horn of the lateral ventricle. The triangular configuration, the local smoothness of the gray-white differentiation and the absence of mass effect, perifocal oedema and contrast enhancement are observed. The differential diagnosis was performed between DNET, GG, FCD IIb.

Visualisation of FCD associates (FCD IIIb by ILAE classification of FCD, 2011 [8]). The results of the MRI under the epileptic scanning protocol, which can reveal additional signs in the form of a trans-mantle sign, local or regional peritumoral gyrus distortion, changes in signal characteristics and alterations of gray-white demarcation (c, d) seem to be the most informative. On preoperative dynamic control, significant changes in the size and shape of the lesions were not identified. (d) In the case of DNET, in addition to the triangular configuration and ‘comet tail’ symptom, the multicystic structure of the lesion with the presence of the primary cyst is observed.

Imaging of diffusely growing glial tumours of Grade I-II. (e, f) Diffuse astrocytomas (DAs) on left temporal lobes in patients with temporal epilepsy show the smoothness of gray-white differentiation, absence of perifocal oedema and insignificant mass-effect. At the first stage on a routine examination, and in the absence of contrast enhancement, DAs can mimic GG or DNET growing diffusely. On the follow-up observation over the next 6–12 months, a progression of the tumour size and increase of perifocal oedema were noticed.

In the diagnosis on admission, the neoplastic process was not mentioned in twelve of the cases and these seem to be the most interesting. All of the patients presented without the typical neuroradiological markers of the neoplastic process and in most cases epileptic seizures were the only clinical symptom (Fig. 2, Fig. 6c, d). Most often, the consequences of hypoxic-ischaemic

injury (including cerebral vascular accidents in the past) and neuroinfections were included in the differential diagnosis (Tab. 1).

For some patients, the follow-up from the onset of epilepsy and the detection of abnormalities on the MRI before the verification of the neoplastic process took more than five years.

It should be noted that in the cases of focal intracortical lesions with uncertain origin, especially when they were located in regions inaccessible for routine MRI, the epileptic scanning protocol was especially helpful for differential diagnosis. In a number of patients, the peculiar visualisation patterns were detected and helped to make a differential diagnosis between DNET, GG, FCD IIb, as described above.

In conclusion, the case histories of two patients are discussed. In the first case, the patient presented with an initial (on admission) diagnosis of FCD IIb, and in the second case the patient presented with an initial diagnosis of a brain tumour; both patients developed epilepsy leading to neurosurgical intervention.

Patient B., male aged 16 years.

Initial (on admission) diagnosis: focal cortical dysplasia of the left temporal lobe. Symptomatic epilepsy, drug-resistant form. A routine MRI performed at the patient's local clinic revealed specific signs of FCD IIb in the left temporal lobe, described in the literature (Fig. 7). On admission, clinical manifestations were observed as focal tonic-automotor seizures with a transition to tonic-clonic seizures, with a frequency of up to six episodes per week. The onset of epilepsy was noted at the age of 12 years, and in the neurological status there were no significant abnormalities throughout the period of preoperative follow-up.

A gradual progression of the regional epileptiform discharges index in the left temporal region in the form of acute-slow wave complexes in the structure of regional slowing down was observed. For several years, the epileptologist at the patient's local clinic has indicated antiepileptic drugs (AED) with repeated changes of dosages and combinations of AEDs. The child was repeatedly examined and treated in the regional Children's Clinical Hospital.

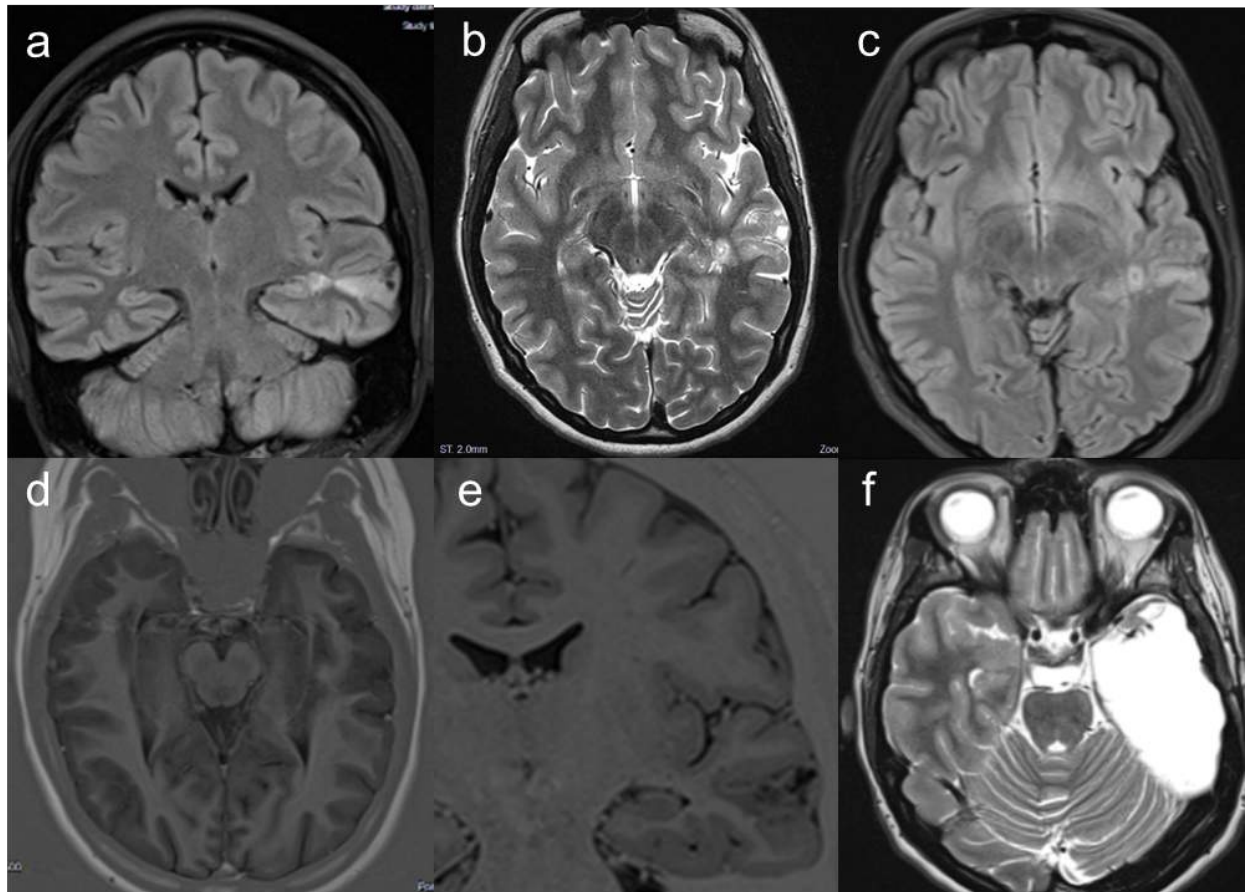


Figure 7. Patient B., male aged 16 years.

Top row: Routine MRI 1.5 T. (a, b) In the cortical-subcortical area in the posterior-lateral parts of the left temporal lobe, the zone of the pathological signal in T2 and FLAIR WI can be seen. There are no signs of perifocal oedema, any mass effect or contrast enhancement. (c) A triangular configuration of the lesion, the presence of the trans-mantle sign and the local disorganisation of the cortical plate, typical for FCD IIb, are visible.

Bottom row. A high resolution MRI on the epilepsy scan protocol with hippocampal positioning of slices. (d) In the SPGR WI mode, the regional perifocal perversion of the cortical plate with diffuse thickening can be seen.

(e) In the IR EPI WI mode, the thickening of the cortex of the lateral and basal temporal lobes with the imperfection of gray-white differentiation is clearly determined on coronary slices. Taking into account the configuration of the pathological focus, regional distortion of the cortical plate, and the gray-white differentiation beyond the focus, a possible neuronal-glial tumour associated with FCD IIIb should be included in the differential diagnosis.

(f) In-depth pre-surgical examination results were consulted, and the decision was taken to perform partial surgical resection of the left temporal lobe.

On admission, the drug-resistant focal epilepsy and the results of EEG monitoring beyond the pathological focus according to MRI data were taken into account; in-depth, comprehensive examination was recommended. A high-resolution MRI epileptic scan protocol revealed abnormalities that had been impossible to visualise earlier (Figure 7d, e). Looking at newly identified neuroradiological signs (regional perifocal thickening, distortion of cortical plates and the smoothness of the gray-white demarcation), clinical symptoms and neurophysiological data of examinations, the differential diagnosis was made between FCD type IIb and FCD IIIb associated with a neuronal-glial tumour.

After considering the results of video-EEG monitoring on a 10-10 system it was jointly decided to perform surgery under the control of ECoG. The patient underwent partial resection of the temporal lobe (Fig. 7f). Histological diagnosis: the morphological picture corresponds to the diagnosis of the combined FCD form IIIb (ILAE classification of FCD, 2011 [8]), and the microscopic tumour foci revealed mostly correspond with ganglioglioma Grade I. However, small amounts of the tumour tissue, anamnesis data, do not allow exclusion of DNET with ganglioglioma Grade I. In accordance with the Engel scale, the outcome is determined as Ia. The period of preoperative follow-up was four years. Postoperative follow-up at the time of writing this article is three years.

Patient S., female aged eight years.

The initial diagnosis was a tumour of the right frontal lobe with symptomatic epilepsy. The epileptic seizures first appeared at the age of six. A MRI was performed at the patient's local clinic and the conclusion was the following: mass lesion in the right frontal lobe, probably of a glial type (Fig. 8a, b, c). The patient was admitted to the Neurosurgery Department of the Russian Children's Clinical Hospital for an examination and immediate choice of treatment strategy.

During the pre-surgical assessment, a MRI (3.0 T) was performed according to the epileptic scanning protocol with the inclusion of a non-contrast MRI perfusion of ASL (arterial spin-labeled) as part of a complex pre-surgical examination. Based on the MRI data, there were some doubts about the neoplastic nature of the pathological focus (Fig. 8d, e).

During the surgery, a differential diagnosis was conducted between the tumour and FCD II type. After the detailed analyses of the results of neuroradiological and neurophysiological assessments, it was decided to perform a focal resection of the pathological formation under ECoG control.

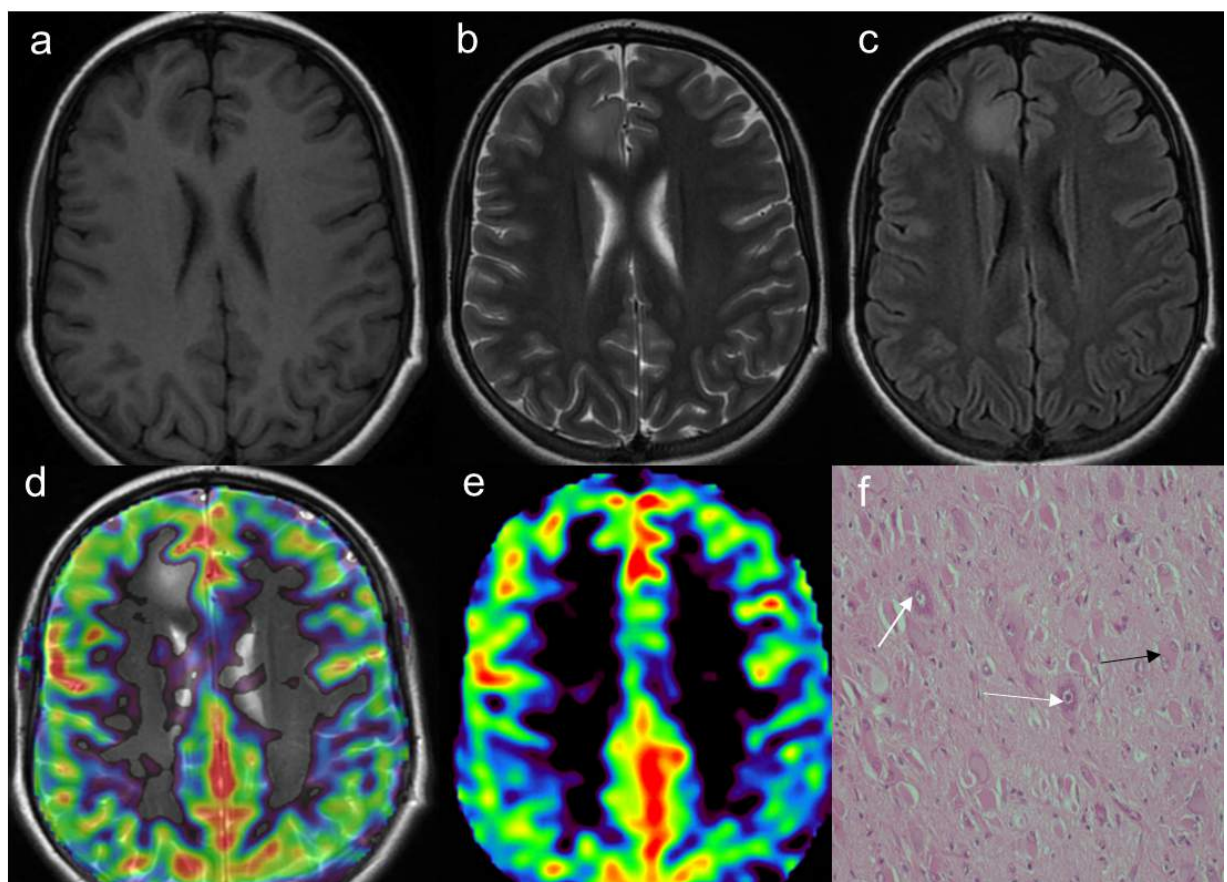


Figure 8. Patient S., female aged eight years.

Top row: (a, b, c) With routine MRI data, the cortical-subcortical zone of the pathological signal in the parasagittal parts of the right frontal lobe is determined; the signal is associated with local distortion of the gyrus architectonics, the lack of mass effect, dynamic transformation and contrast enhancement.

Inside the pathological area, there is a rounded inclusion with more intense signal characteristics in T2 and T1 WI. Also, according to the routine images data, it seems that there is a (b, c) perifocal oedema around a more intense inclusion according to T2 and FLAIR data. This was regarded as a solid component of the tumour.

Bottom row: At the same time, according to ASL data, regional iso/hypoperfusion coinciding with the assessing zone (scale in d) is determined, which (e,f) leads the differential diagnosis in favour of the dysplastic origin of changes or a FCD-associated tumour of FCD IIIb type with the dysplastic component predominance. Post-surgery, the Anatomic Pathology Department confirmed the histological picture of FCD type IIb, (e) using hematoxylin and eosin x 200 for staining. (f) Dysmorphic neurons are shown with white arrows and balloon cells are shown with black arrows.

Histological diagnosis

Brain tissue fragments demonstrate the abnormal radial and tangential lamination of the cortex. The demarcation of gray and white matter is distorted, large balloon-like cells can be determined in the white matter – some of them containing two nuclei – and there are also dysmorphic neurons (Fig. 8e, f). The picture corresponds to FCD IIb type (ILAE classification of FCD, 2011 [8]). The period of preoperative follow-up was eight months. Postoperative follow-up is 1.5 years. Outcome on the Engel scale is IIa.

Table 1. The Patients' Assessments Results

Histological type of the lesion	Number of patients	Location of the lesion	Confirmed FCD-associates/ composite tumour	Differential diagnosis
Dysembryoplastic neuroepithelial tumours (DNET)	18 patients	Temporal – 9 Parietal – 3 Frontal – 3 Multilobar – 2	4 cases: 3 cases – DNET in FCDIIIb 1 case – DNET + GG	Hypoxic-ischaemic injury – 3 CNS infection – 2 Current CNS infection – 1 Arachnoid cyst – 1
Gangliogliomas (GG)	15 patients	Temporal – 7 Parietal – 2 Frontal – 2 Multilobar – 3	2 cases: 1 case – GG in FCDIIIb 1 case – GG + DNET in FCDIIIb	Hypoxic-ischaemic injury – 1 CNS infection – 1 Parasites – 1 Arachnoid cyst – 2
Total	33 patients	16 patients	6 patients	12 patients

Table 2. Specific DNET and GG patterns on the MRI

Histological type	Number	'Soap bubble'	Main cyst	Triangle pattern	Tract intact	Local changes of the bone tissue	Comet tail (trans mantle)	Presence of 2 or more signs
DNET	18	11	3	12	4	2	3	13
GG	15	7	7	8	2	4	–	8
Total	33	18	10	17	6	6	3	21

Discussion

Some particularities to be found in DNET and GG visualisation are shown in our study. Usually on the routine MRIs it is often difficult to distinguish them from low-differentiated tumours like diffuse astrocytomas Grade I-II, oligodendrogliomas and pleomorphic xanthoastrocytomas [10, 11]. The differential diagnosis is extremely important as these more aggressive tumours as a rule require complex treatment, including radiation and chemotherapy in addition to surgery. On the other hand, DNETs and GGs are incredibly stable tumours, which can be operated on mostly for drug-resistant epilepsy, as mentioned above. Surgical treatment of epilepsy in DNET and GG requires an in-depth preoperative preparation involving identification of the epileptogenic lesion, which can be protracted significantly beyond the area of MRI visualising abnormalities if these tumours are representing a part of brain congenital anomalies complex, so they can be called ‘tip of the iceberg’ [12].

The most common neuroradiological sign of DNET and GG is the ‘soap bubble’ pattern as well as the ‘triangular’ shape of the lesion. Also, the following terms are used: ‘alveolar type’ and ‘foam-like structure’, represented by local accumulations of intracortical microcysts which are divided by septal structures into chambers [2, 13].

GGs can be represented by clearly demarcated cystic components (sometimes mimicking cortical congenital arachnoid cysts), where a solid tumour can be missed (Fig. 2a, b).

Quite often the main cyst, surrounded by multicysts of smaller sizes, can be seen [5, 13]. These microcyst clusters are clearly visible on the images in the T2, FLAIR and T1 WI modes; SPGR (fast cleaned gradients) is considered to be the optimal mode of scanning (Fig. 5h; 7g, h).

The triangular pattern is characterised by a local area of MR signal enhancement in T2 and FLAIR WI, widest at the cortical level, wedging into the white matter and narrowing towards the horns of the lateral ventricle (Fig. 3). It is believed that DNETs and GGs have a dysembryoplastic origin, so a triangular distribution form can be caused by the radial arrangement of glial fibres [2, 14]. That is the rather specific pattern for DNET to be found in most cases.

Besides DNETs and GGs, the ‘soap bubble’ sign can occur in oligodendrogliomas and xanthoastrocytomas which may also have a cortical localisation and multicystic structure, but tend to have aggressive growth with contrast enhancement, mass effect, infiltration of the adjacent meninges, and peritumoral oedema of varying severity [10, 11, 15].

Other glial-cystic lesions, due to the consequences of vascular accidents and CNS infections, can mimic the multicystic structure of DNET and GG, if they are localised in the subcortical regions and involve the temporo-insular cortical regions.

But as a rule, correlating the medical history, laboratory findings and follow-up data make it possible to differentiate these processes, because they are susceptible to continued transformation. In our study, a triangular configuration was more often associated with DNETs than with GGs or FCD IIb type. Considering the similar clinical manifestations, the above patterns should be taken into account when a differential row is being constructed. In some cases, FCD IIb types have pseudocysts in their structure, are of intracortical localisation and tend to be of a triangular shape [12, 16]. In addition, DNETs and GGs had their foundation in the basement membrane of the cortex, and their tip extended towards the lateral ventricle, forming the so-called ‘comet tail’ [15, 17].

On MRI visualisation, these abnormalities are similar to the ‘trans mantle’ pattern, considered to be a highly specific sign of FCD IIb [12, 18]. This issue didn't allow us to make a definite decision in favour of any process in the differential row of DNET, GG and FCD IIb. DTI and FA were used in some patients in the preoperative stage to determine the histopathological and expanding characteristics of the tumours, along with the degree of their malignancy.

Some authors note the main type of impact on the pathways, such as divergence, displacement, infiltration or oedema [15, 19, 20]. In our study, the DTI data tended to indicate displacement (in six cases) rather than the divergence of the fibres, while according to the FA, the integrity of the fibres was not disrupted; this, in turn, indicated the less aggressive nature of the tumour.

As DNETs grow, the remodeling of the adjacent bone tissue can often be seen on neuroimaging. In many cases, taking into account clinical and neuroimaging similarities with FCD IIb, this sign can be considered as a reliable neuroradiological marker for neoplastic process verification, as well as the contrast enhancement [15, 21]. The contrast enhancement is possible if the glial component dominates the neuronal component in the mass structure.

In accordance with the literature data, an association with FCD IIIb dysplasia is found in approximately 50% of cases [15, 22]. The lower percentage in our study (in six out of 33 cases the association of neuronal-glioma tumours with FCD type IIIb was revealed and histopathologically confirmed, which corresponds to 18%) could be explained by the fact that we have relatively recently gained access to appropriate and up-to-date histological diagnostic technologies. To specify the individual assessment protocol for a particular patient, the counsel of experts was used, including epileptologists and neurophysiologists for the interpretation of the EEG results.

Based on the results of the experts' counsel examination, a complex pre-operative assessment was recommended to 21 patients. This comprehensive assessment included high resolution MRI with the methods for determining the seizure onset zone and mapping the significant functional cortical areas (subdural invasive video-EEG monitoring, WADA test, PET with methionine, functional MRI). The use of intraoperative ECoG to remove or deafferentate the cortex area, the activity which initiates the seizure (the epileptogenic zone) is mandatory.

Conclusions

Specific MRI patterns described in the literature as DNET characteristics, can be revealed in patients with GGs and FCD IIb (balloon-cell) type. It is not possible to differentiate DNET from GG and FCD IIb in a conclusive way based on the standard MRI even in the presence of three or more of the above-described specific signs.

Despite the similarities of neuroimaging characteristics of DNETs and GGs in some cases, the latter have a greater tendency to show malignant transformation and recurrence.

In the presence of a cortical epileptogenic substrate of unknown etiology, it is necessary to apply a comprehensive in-depth pre-surgical assessment. The main objectives of neuroimaging are verification of a benign neoplastic process, determination of the true size of the mass and the most accurate localisation, all of which directly determine the tactics of epileptic surgery.

Along with the introduction of high-resolution super inductive MRI systems, application of modern complex research protocols, including pulse sequences, T2 PROPELLER, FLAIR in the axial and coronal planes, FSPGRBRAVO, T1 SE, DWI, SWAN, DTI and ASL-perfusion are of great importance, but above all there is a high qualification of a neuroradiologist.

When evaluating the masses to be operated on, a correct and accurate sample of material to be studied (not only from the primary tumour substance, but also from the adjacent dysplastic tissues, including the area of trans-mantle migration abnormalities), as well as the examination of histological specimens made by a highly qualified pathomorphologist are of great importance. The aim of surgical intervention in dysembryoplastic brain tumours is not only treatment for a patient for the tumour and minimising the risk of possible malignant transformation and recurrence, but also the removal of epileptogenic substrates. This leads to favourable postoperative outcomes according to the Engel classification, and this will eventually improve the patients' quality of life.

Competing interests

The authors have declared that no competing interest exists.

Acknowledgements

The authors are grateful for the advice and support of the staff at the Radiology Department of the Russian Children's Clinical Hospital in Moscow, especially the Head of the Department, Professor A.A. Alikhanov.

This is an Open Access article distributed under the terms of the Creative Commons Attribution License (<https://creativecommons.org/licenses/by-nc-sa/4.0/>), which permits unrestricted use, distribution, and reproduction in any medium, provided the original work is properly credited. The Creative Commons Public Domain Dedication waiver (<http://creativecommons.org/publicdomain/zero/1.0/>) applies to the data made available in this article, unless otherwise stated.

References

1. García-Fernández M, Fournier-Del Castillo C, Ugalde-Canitrot A, Pérez-Jiménez Á, Álvarez-Linera J, De Prada-Vicente I | display-authors=etal (2011) [Epilepsy surgery in children with developmental tumours](#). *Seizure* 20 (8):616-27. DOI: [10.1016/j.seizure.2011.06.003](https://doi.org/10.1016/j.seizure.2011.06.003) PMID: [21741275](https://pubmed.ncbi.nlm.nih.gov/21741275/).
2. Fernandez C, Girard N, Paz Paredes A, Bouvier-Labit C, Lena G, Figarella-Branger D (2003) [The usefulness of MR imaging in the diagnosis of dysembryoplastic neuroepithelial tumor in children: a study of 14 cases](#). *AJNR Am J Neuroradiol* 24 (5):829-34. PMID: [12748079](https://pubmed.ncbi.nlm.nih.gov/12748079/).
3. Stepanenko AIu, Arkhipova NA, Shishkina LV, Pronin IN, Lubnin AIu, Buklina SB (2008) [\[Surgical tactics for the treatment of symptomatic temporal lobe epilepsy\]](#). *Zh Vopr Neurokhir Im N N Burdenko* (1):17-22. PMID: [18488891](https://pubmed.ncbi.nlm.nih.gov/18488891/).
4. Urbach H (2008) [MRI of long-term epilepsy-associated tumors](#). *Semin Ultrasound CT MR* 29 (1):40-6. DOI: [10.1053/j.sult.2007.11.006](https://doi.org/10.1053/j.sult.2007.11.006) PMID: [18383906](https://pubmed.ncbi.nlm.nih.gov/18383906/).
5. Khalilov VS, Kholin AA, Medvedeva NA, Rasskazchikova IV, Bobylova MY, Zavadenko NN (2017) [\[The use of low-field MRI for visualization of epileptogenic brain lesions in children\]](#). *Zh Nevrol Psikhiatr Im S S Korsakova* 117 (11):84-90. DOI: [10.17116/jnevro201711711184-90](https://doi.org/10.17116/jnevro201711711184-90) PMID: [29265092](https://pubmed.ncbi.nlm.nih.gov/29265092/).
6. Khalilov V.S., Kholin A.A., Kostylev F.A., Balyulin Yu.V., Gubachikova F.A., Gazdieva Kh.Sh. Specific MRI-patterns of neuronal-glia tumors associated with focal epilepsy in children. *Radiological Diagnostics and Therapy* 2017; 2(8): 63-64. (in Russ.)
7. Prayson RA, Napekoski KM (2012) [Composite ganglioglioma/dysembryoplastic neuroepithelial tumor: a clinicopathologic study of 8 cases](#). *Hum Pathol* 43 (7):1113-8. DOI: [10.1016/j.humpath.2011.08.023](https://doi.org/10.1016/j.humpath.2011.08.023) PMID: [22221701](https://pubmed.ncbi.nlm.nih.gov/22221701/).
8. Blümcke I, Thom M, Aronica E, Armstrong DD, Vinters HV, Palmini A | display-authors=etal (2011) [The clinicopathologic spectrum of focal cortical dysplasias: a consensus classification proposed by an ad hoc Task Force of the ILAE Diagnostic Methods Commission](#). *Epilepsia* 52 (1):158-74. DOI: [10.1111/j.1528-1167.2010.02777.x](https://doi.org/10.1111/j.1528-1167.2010.02777.x) PMID: [21219302](https://pubmed.ncbi.nlm.nih.gov/21219302/).
9. Phi JH, Kim SK, Cho BK, Lee SY, Park SY, Park SJ | display-authors=etal (2009) [Long-term surgical outcomes of temporal lobe epilepsy associated with low-grade brain tumors](#). *Cancer* 115 (24):5771-9. DOI: [10.1002/cncr.24666](https://doi.org/10.1002/cncr.24666) PMID: [19806640](https://pubmed.ncbi.nlm.nih.gov/19806640/).
10. Koeller KK, Henry JM (2001) [From the archives of the AFIP: superficial gliomas: radiologic-pathologic correlation](#). *Armed Forces Institute of Pathology. Radiographics* 21 (6):1533-56. DOI: [10.1148/radiographics.21.6.g01nv051533](https://doi.org/10.1148/radiographics.21.6.g01nv051533) PMID: [11706224](https://pubmed.ncbi.nlm.nih.gov/11706224/).

11. Khalilov VS, Kholin AA, Medvedeva NA, Vasiliev IG, Rasskazchikova IV, Ismailova RR | display-authors=etal (2016) [\[MRI-characteristics of epileptogenic supratentorial brain tumors in children\]](#). Zh Nevrol Psikhiatr Im S S Korsakova 116 (1):56-63. DOI: [10.17116/jnevro20161161156-63](#) PMID: [26977627](#).
12. Daumas-Duport C, Varlet P, Bacha S, Beuvon F, Cervera-Pierot P, Chodkiewicz JP (1999) [Dysembryoplastic neuroepithelial tumors: nonspecific histological forms -- a study of 40 cases.](#) J Neurooncol 41 (3):267-80. DOI: [10.1023/a:1006193018140](#) PMID: [10359147](#).
13. Suh YL (2015) [Dysembryoplastic Neuroepithelial Tumors.](#) J Pathol Transl Med 49 (6):438-49. DOI: [10.4132/jptm.2015.10.05](#) PMID: [26493957](#).
14. Lee DY, Chung CK, Hwang YS, Choe G, Chi JG, Kim HJ | display-authors=etal (2000) [Dysembryoplastic neuroepithelial tumor: radiological findings \(including PET, SPECT, and MRS\) and surgical strategy.](#) J Neurooncol 47 (2):167-74. DOI: [10.1023/a:1006401305247](#) PMID: [10982159](#).
15. Paudel K, Borofsky S, Jones RV, Levy LM (2013) [Dysembryoplastic neuroepithelial tumor with atypical presentation: MRI and diffusion tensor characteristics.](#) J Radiol Case Rep 7 (11):7-14. DOI: [10.3941/jrcr.v7i11.1559](#) PMID: [24421925](#).
16. Kabat J, Król P (2012) [Focal cortical dysplasia - review.](#) Pol J Radiol 77 (2):35-43. DOI: [10.12659/pjr.882968](#) PMID: [22844307](#).
17. Parmar HA, Hawkins C, Ozelame R, Chuang S, Rutka J, Blaser S (2007) [Fluid-attenuated inversion recovery ring sign as a marker of dysembryoplastic neuroepithelial tumors.](#) J Comput Assist Tomogr 31 (3):348-53. DOI: [10.1097/01.rct.0000243453.33610.9d](#) PMID: [17538277](#).
18. Mukhin K.Yu. FOCAL CORTICAL DYSPLASIAS: CLINICAL AND ELECTRO-NEUROIMAGING CHARACTERISTICS. Russian Journal of Child Neurology. 2016;11(2):8-24. (In Russ.) <https://doi.org/10.17650/2073-8803-2016-11-2-8-24>
19. Yen PS, Teo BT, Chiu CH, Chen SC, Chiu TL, Su CF (2009) [White Matter tract involvement in brain tumors: a diffusion tensor imaging analysis.](#) Surg Neurol 72 (5):464-9; discussion 469. DOI: [10.1016/j.surneu.2009.05.008](#) PMID: [19608227](#).
20. Wei CW, Guo G, Mikulis DJ (2007) [Tumor effects on cerebral white matter as characterized by diffusion tensor tractography.](#) Can J Neurol Sci 34 (1):62-8. DOI: [10.1017/s0317167100005801](#) PMID: [17352349](#).
21. Alikhanov A.A., Ryzhkov B.N., Demushkina A.A. Vizualization of dysplastic brain substrates in epileptic children. Neurosurgery and neurology of childhood. 2010; 1(23): 27-38. (In Russ.)
22. Frater JL, Prayson RA, Morris III HH, Bingaman WE (2000) [Surgical pathologic findings of extratemporal-based intractable epilepsy: a study of 133 consecutive resections.](#) Arch Pathol Lab Med 124 (4):545-9. DOI: [10.5858/2000-124-0545-SPFOEB](#) PMID: [10747311](#).